

## Two finite-difference schemes for calculation of Bingham fluid flows in a cavity

E. A. MURAVLEVA\* and M. A. OLSHANSKII\*

**Abstract** — Two finite-difference schemes are proposed in the paper for the calculation of a viscous incompressible Bingham fluid flow. The Duvaut–Lions variational inequality is considered as a mathematical model of the medium. One of the finite-difference schemes is a generalization of the well-known MAC scheme on staggered grids. The other scheme uses one grid for approximation of all velocity components and another grid for all components of the rate of deformation tensor and pressure. A special stabilizing term is introduced into this scheme, which provides stability and preserves the second order of convergence of the scheme. Additional consistency conditions for grid operators are introduced, which are necessary for the correctness of the difference method. The numerical solution of the problem of the Bingham fluid flow in a cavity is considered as a model example.

### 1. Introduction

There are many materials in nature and industry exhibiting the behaviour of the Bingham medium. For example, these are fresh concrete, geomaterials (argillaceous soil, oil-bearing materials, mudflow, magma), colloid solutions, powder mixtures, lubricants, metals under pressure treatment, blood in a capillary, foodstuffs, toothpaste. Such medium below a certain stress value behaves as a rigid body and above this level behaves as an incompressible fluid. Therefore, construction of efficient numerical methods for the calculation of Bingham media flows is an important problem attracting the attention of many researches (see, e.g., [8] and the references therein).

Let  $\Omega$  be a bounded connected domain in  $R^n, n = 2, 3$ ,  $\Gamma$  be the boundary of the domain. The isothermal flow of an incompressible visco-plastic medium (Bingham medium or Bingham fluid) during the time interval  $(0, T)$  is described by the following system of equations and constitutive relations:

$$\rho \left[ \frac{\partial \mathbf{v}}{\partial t} + (\mathbf{v} \cdot \nabla) \mathbf{v} \right] = \operatorname{div} \cdot \boldsymbol{\sigma} + \mathbf{f} \quad \text{in } \Omega \times (0, T) \quad (1.1)$$

$$\nabla \cdot \mathbf{v} = 0 \quad \text{in } \Omega \times (0, T) \quad (1.2)$$

---

\*Moscow M. V. Lomonosov State University, Moscow 119992, Russia

The work was supported by the Russian Foundation for Basic Research and Deutsche Forschungsgemeinschaft (08-01-00159, 06-01-04000).

the Cauchy stress tensor  $\boldsymbol{\sigma}$  can be written down as

$$\boldsymbol{\sigma}_{ij} = -p \cdot \delta_{ij} + \boldsymbol{\tau}_{ij}$$

where  $p$  is the pressure,  $\boldsymbol{\tau}$  is the stress tensor satisfying the relations

$$\begin{aligned} \tau_{ij} &= 2\mu D_{ij}(\mathbf{v}) + \tau_s \frac{D_{ij}(\mathbf{v})}{|\mathbf{D}(\mathbf{v})|}, & |\mathbf{D}(\mathbf{v})| &\neq 0 \\ |\boldsymbol{\tau}| &\leq \tau_s, & |\mathbf{D}(\mathbf{v})| &= 0. \end{aligned} \quad (1.3)$$

System (1.1)–(1.3) has to be supplied with initial and boundary conditions. For the sake of simplicity, we consider only the Dirichlet boundary conditions:

$$\mathbf{v}(0) = \mathbf{v}_0 \quad \text{in } \Omega, \quad \nabla \cdot \mathbf{v}_0 = 0 \quad (1.4)$$

$$\mathbf{v} = \mathbf{v}_B \quad \text{on } \Gamma \times (0, T), \quad \int_{\Gamma} \mathbf{v}_B(t) \cdot \mathbf{n} \, d\Gamma = 0 \quad \forall t \in (0, T) \quad (1.5)$$

where  $\mathbf{n}$  is the outward unit normal vector at  $\Gamma$ . Equations (1.1)–(1.5) utilize the standard notations:  $\rho$  and  $\mu$  are positive constants ( $\rho$  is density and  $\mu$  is the viscosity coefficient),  $\tau_s \geq 0$  is the yield stress of the Bingham medium,  $\mathbf{v}$  is the unknown velocity field,  $\mathbf{f}$  is the given field of external forces,  $\mathbf{D}(\mathbf{v}) = (1/2) [\nabla \mathbf{v} + (\nabla \mathbf{v})^T]$  is the rate of deformation tensor and

$$|\mathbf{D}(\mathbf{v})| = \left( \sum_{1 \leq i, j \leq n} |D_{ij}(\mathbf{v})|^2 \right)^{1/2}.$$

Note that if  $\tau_s = 0$ , system (1.1)–(1.5) is reduced to the Navier–Stokes system modelling the isothermal flow of an incompressible viscous Newtonian fluid. In the case  $\tau_s > 0$  system (1.1)–(1.5) holds in the flow domain (i.e.,  $\mathbf{D}(\mathbf{v}) > 0$ ) and, generally speaking, has no sense in the rigid zone  $\Omega_0$ :

$$\Omega_0 = \{ \{\mathbf{x}, t\} \in \Omega \times (0, T) \mid \mathbf{D}(\mathbf{v})(\mathbf{x}, t) = 0 \}. \quad (1.6)$$

Constitutive relations (1.3) are equivalent to the following:

$$D_{ij}(\mathbf{v}) = \begin{cases} \left(1 - \frac{\tau_s}{|\boldsymbol{\tau}|}\right) \frac{\tau_{ij}}{2\mu}, & |\boldsymbol{\tau}| > \tau_s \\ 0, & |\boldsymbol{\tau}| \leq \tau_s. \end{cases}$$

If  $\tau_s > 0$ , then the flow may have zones where the medium behaves as a rigid body (rigid zones). For an increasing  $\tau_s$  these zones expand and for a sufficiently large  $\tau_s$  block the flow. If both flow types exist, we can speak of the presence of a ‘yield surface’. This surface divides two domains with different types of the motion of material.

Thus, a special character of visco-plastic flow problems is the need to solve equations in domains with unknown boundaries. This fact complicates the construction of efficient methods. The main difficulty in numerical simulation of a visco-plastic flow is connected with the singularity of relations (1.3) and impossibility to determine stresses in the domains where the rate of deformation equals zero. In order to overcome these difficulties, various modifications (regularizations) of the Bingham medium model have been introduced. For example, the medium is considered as a nonlinear viscous fluid (without a yield surface):

$$\tau_{ij} = \eta_\varepsilon(|\mathbf{D}|)D_{ij}, \quad \varepsilon \ll 1$$

where  $\eta_\varepsilon(|\mathbf{D}|) \rightarrow \eta(|\mathbf{D}|)$  for  $\varepsilon \rightarrow 0$ . The most popular models are the Bercovier–Engelman [2]

$$\eta_\varepsilon = 2\mu + \tau_s \left( \frac{1}{[\varepsilon^2 + |\mathbf{D}|^2]^{1/2}} \right)$$

and the Papanastasiou model [20]

$$\eta_\varepsilon = 2\mu + \tau_s \left( \frac{1 - e^{-|\mathbf{D}|/\varepsilon}}{|\mathbf{D}|} \right).$$

Besides the smooth regularized models, a model with piecewise-constant viscosity ('biviscosity') [19] is widely used. The regularized models have shortcomings. Thus, for  $\varepsilon \rightarrow 0$  (i.e., when the model approximates the Bingham medium) numerical methods for regularized models become less efficient and the computation time grows rapidly. Another drawback of a regularized model is the following: if the right-hand side function  $\mathbf{f}$  in (1.1) is less than some nonzero critical value, there is no flow in the domain for the Bingham medium, but in regularized models a flow always exists although with small velocities. In the case of an unsteady problem, a regularized model may represent the behaviour of the solution for  $t \rightarrow \infty$  incorrectly, [8]. Moreover, the notion of a rigid zone is not defined for regularized models and the presence of a rigid zone is introduced by the condition of small deformations or by the Mises condition ( $|\boldsymbol{\tau}| = \tau_s$ ).

One may consider variational methods as alternatives for regularized models. The application of the theory of variational inequalities to problems of Bingham fluid flows was presented in [9]. Numerical methods for solution of variational inequalities for Bingham media have been developed in [12] and [13], these methods are based on a nonregularized Bingham model and Lagrange multipliers. Initially the approach based on regularization was widely used by engineers. One reason is that numerical methods based on variational inequalities require a multiple solution of saddle-point systems for finding an approximate solution to a variational inequality at each time step, whereas a regularized system, which is a less adequate mathematical model of the medium, is suitable for application of splitting schemes. Nevertheless, considerable progress in numerical methods for saddle-point

problems in the past two decades (see, e.g., review [1]) makes the approach based on variational inequalities more and more attractive. The growing interest in this method is confirmed by numerous recent publications, see, e.g., [16, 22, 23, 25–27] and review [8].

Numerical simulation of Bingham media traditionally uses the finite element method for discretization. However, the inclusion of Bingham models (along with other non-Newtonian models of continuous media) as part of hydrodynamic packages requires attention to finite difference and finite volume methods, which are traditional in computational fluid dynamics. In this paper we consider the nonregularized model of the Bingham medium based on variational inequalities. Two difference schemes are constructed for determination of an approximate solution. One of the difference schemes is a generalization of the well-known MAC scheme on staggered grids. The MAC scheme was first proposed for the calculation of Navier–Stokes equations for an incompressible fluid and its description can be found in most books on computational fluid dynamics, see, e.g., [10]. The second scheme uses one grid (the same nodes) for approximation of all components of the velocity and another grid for all components of the rate of deformation tensor and pressure. This scheme is more convenient from the implementation viewpoint and also for specification of boundary conditions. Thus, in the three-dimensional case the first scheme requires to handle data structures on seven different grids, whereas the second scheme requires only two grids. However, the scheme on non-staggered grids is unstable in the sense of Ladyzhenskaya–Babuska–Brezzi. In order to overcome this difficulty, we introduce a special stabilizing term providing stability of the scheme and retaining the second order of convergence in the  $L^2$  norm for the velocity and the first order of convergence in the  $L^2$  norm for the pressure. The stabilized scheme can be used both in the two- and three-dimensional cases.

Note that using a nonregularized Bingham model, it is not quite clear how to apply the finite difference method for approximation of variational inequalities. Therefore, the following approach seems reasonable: first we write down an iterative process for finding the saddle point of the full Lagrangian of the problem in a differential form. Further, we construct finite-difference schemes for discretization of the corresponding auxiliary differential problems appearing at each step of the method. It has been established that an additional condition of the consistency of the difference operators is required for the correctness of the method.

A numerical solution of the Bingham flow problem in a cavity is considered as a model example in the paper. The obtained results (velocity and pressure fields and rigid zones) are in good agreement with those known from the literature.

## 2. Variational statement and iterative process

Duvaut and Lions [9] have proved that any solution to nonlinear system (1.1)–(1.5) satisfies the following variational problem: determine  $\mathbf{v}(t), p(t) \in (H^1(\Omega))^n \times$

$L^2(\Omega)$  so that for each  $t \in (0, T)$  the following relations hold:

$$\begin{aligned} & \rho \int_{\Omega} \frac{\partial \mathbf{v}}{\partial t} \cdot (\mathbf{u} - \mathbf{v}(t)) \, d\mathbf{x} + \rho \int_{\Omega} (\mathbf{v}(t) \cdot \nabla) \mathbf{v}(t) \cdot (\mathbf{u} - \mathbf{v}(t)) \, d\mathbf{x} \\ & + \mu \int_{\Omega} \nabla \mathbf{v}(t) \nabla (\mathbf{u} - \mathbf{v}(t)) \, d\mathbf{x} + \sqrt{2}g \int_{\Omega} (|\mathbf{D}(\mathbf{u})| - |\mathbf{D}(\mathbf{v}(t))|) \, d\mathbf{x} \\ & \geq \int_{\Omega} \mathbf{f}(t) \cdot (\mathbf{u} - \mathbf{v}(t)) \, d\mathbf{x} \quad \forall \mathbf{u} \in \mathbf{U}_B \end{aligned} \quad (2.1)$$

$$\nabla \cdot \mathbf{v}(t) = 0 \quad \text{in } \Omega \quad (2.2)$$

$$\mathbf{v}(0) = \mathbf{v}_0 \quad (2.3)$$

$$\mathbf{v}(t) = \mathbf{v}_B(t) \quad \text{on } \Gamma \quad (2.4)$$

$$\mathbf{U}_B = \{ \mathbf{u} \in (H^1(\Omega))^n \mid \mathbf{u} = \mathbf{v}_B \text{ on } \Gamma, \nabla \cdot \mathbf{u} = 0 \}. \quad (2.5)$$

It was also shown there that the solution to (2.1)–(2.5) may be formally considered as the solution to (1.1)–(1.5). Thus, problem (2.1)–(2.5) is the variational statement for (1.1)–(1.5) and in this case it automatically includes the problem on the yield surface. The pressure can be introduced into the variational statement as a Lagrange multiplier corresponding to the restriction  $\nabla \cdot (\mathbf{u} - \mathbf{v}(t)) = 0$ .

Suppose the flow is stationary and slow, i.e., we can neglect the convective terms and the terms including  $\partial \mathbf{v} / \partial t$ . Then the variational statement takes the form

$$\mu \int_{\Omega} \nabla \mathbf{v} : \nabla (\mathbf{u} - \mathbf{v}) \, d\mathbf{x} + \tau_s \int_{\Omega} |\mathbf{D}(\mathbf{u})| - |\mathbf{D}(\mathbf{v})| \, d\mathbf{x} \geq \int_{\Omega} \mathbf{f} \cdot (\mathbf{u} - \mathbf{v}) \, d\mathbf{x} \quad \forall \mathbf{u} \in \mathbf{U}_B \quad (2.6)$$

$$\nabla \cdot \mathbf{v} = 0 \quad (2.7)$$

$$\mathbf{v} = \mathbf{v}_B \quad \text{on } \Gamma. \quad (2.8)$$

Introduce the following functional:

$$J(\mathbf{u}) = \mu \int_{\Omega} |\mathbf{D}(\mathbf{u})|^2 \, d\mathbf{x} + \tau_s \int_{\Omega} |\mathbf{D}(\mathbf{u})| \, d\mathbf{x} - 2 \int_{\Omega} \mathbf{f} \cdot \mathbf{u} \, d\mathbf{x}.$$

It was proved in [9] that the solution  $\mathbf{v}$  to problem (2.6)–(2.8) is the minimum point of the functional  $J$  on  $\mathbf{U}_B$ :

$$\mathbf{v} = \arg \min_{\mathbf{u} \in \mathbf{U}_B} J(\mathbf{u}).$$

The main difficulty in finding the numerical solution to variational problem (2.6)–(2.8) is the nondifferentiability of the term  $\int_{\Omega} |\mathbf{D}(\mathbf{v})| \, d\mathbf{x}$ . Several ways to overcome this difficulty were proposed in [12]. The method of Lagrange multipliers is widespread. The basic idea of this approach consists in separation of ‘nonlinearity’ and ‘differentiation’ performed in the following way. Introduce an independent variable  $\boldsymbol{\gamma} = \mathbf{D}(\mathbf{v}) \in Q$ , where  $Q = \{ \mathbf{q} \mid \mathbf{q} \in (L^2(\Omega))^{n \times n}, \mathbf{q}^T = \mathbf{q} \}$ . Define the Lagrangian

$$\mathcal{L}(\mathbf{v}, \boldsymbol{\gamma}, \boldsymbol{\tau}) = \mu \int_{\Omega} |\boldsymbol{\gamma}|^2 \, d\mathbf{x} + \tau_s \int_{\Omega} |\boldsymbol{\gamma}| \, d\mathbf{x} + \int_{\Omega} (\mathbf{D}(\mathbf{v}) - \boldsymbol{\gamma}) : \boldsymbol{\tau} \, d\mathbf{x} - 2 \int_{\Omega} \mathbf{f} \cdot \mathbf{v} \, d\mathbf{x}$$

where  $\boldsymbol{\tau} \in Q$  is the Lagrange multiplier corresponding to the restriction  $\boldsymbol{\gamma} = \mathbf{D}(\mathbf{v})$ ,  $\boldsymbol{\tau}$  can be interpreted as the deviator of the stress tensor. Then the solution  $\mathbf{v}$  is the saddle point of  $\mathcal{L}$ , i.e., it is the solution to the problem

$$\min_{\boldsymbol{\gamma}, \mathbf{v}} \max_{\boldsymbol{\tau}} \mathcal{L}(\mathbf{v}, \boldsymbol{\gamma}, \boldsymbol{\tau}).$$

For some fixed  $\boldsymbol{\tau}$  and  $\boldsymbol{\gamma}$ , the Lagrangian is not coercitive with respect to the variable  $\mathbf{v}$ . Therefore, in calculations we use the penalty method with respect to the restriction  $\boldsymbol{\gamma} - \mathbf{D}(\mathbf{v}) = 0$ . To do that, define the extended Lagrangian  $\mathcal{L}_r : (H^1(\Omega))^2 \times Q \times Q \rightarrow \mathbb{R}$

$$\mathcal{L}_r(\mathbf{v}, \boldsymbol{\gamma}, \boldsymbol{\tau}) = \mathcal{L}(\mathbf{v}, \boldsymbol{\gamma}, \boldsymbol{\tau}) + r \int_{\Omega} |\mathbf{D}(\mathbf{v}) - \boldsymbol{\gamma}|^2 dx, \quad r \geq 0. \quad (2.9)$$

The extended Lagrangian is coercitive with respect to  $\mathbf{v}$  for all  $r > 0$ . Therefore, for fixed  $\boldsymbol{\tau}$  and  $\boldsymbol{\gamma}$  we can minimize  $\mathcal{L}_r$  over  $\mathbf{v}$  on  $\mathbf{U}_B$  in spite of the fact that this operation is practically impossible for  $r = 0$ . For solution of problem (2.6)–(2.8), an iterative method was proposed in [13] for determination of the saddle point of  $\mathcal{L}_r$ . The algorithm presented below can be considered as an analogue of Uzawa's method for linear problems with a saddle point.

Let arbitrary  $\boldsymbol{\gamma}^0, \boldsymbol{\tau}^0$  be given. For  $n = 0, 1, 2, \dots$  we successively perform the following steps. Determine  $\mathbf{v}^{n+1} \in \mathbf{U}_B$  so that

$$\mathcal{L}_r(\mathbf{v}^{n+1}, \boldsymbol{\gamma}^n, \boldsymbol{\tau}^n) \leq \mathcal{L}_r(\mathbf{u}, \boldsymbol{\gamma}^n, \boldsymbol{\tau}^n) \quad \forall \mathbf{u} \in \mathbf{U}_B.$$

Further, find  $\boldsymbol{\gamma}^{n+1}$  so that

$$\mathcal{L}_r(\mathbf{v}^{n+1}, \boldsymbol{\gamma}^{n+1}, \boldsymbol{\tau}^n) \leq \mathcal{L}_r(\mathbf{v}^{n+1}, \boldsymbol{\mu}, \boldsymbol{\tau}^n) \quad \forall \boldsymbol{\mu} \in Q.$$

Finally, set

$$\boldsymbol{\tau}^{n+1} := \boldsymbol{\tau}^n + 2\tilde{r}_n(\mathbf{D}(\mathbf{v}^{n+1}) - \boldsymbol{\gamma}^{n+1}). \quad (2.10)$$

Using variational analysis, the algorithm can be rewritten in the following form (see [13]).

**Algorithm (A):**

Step 1. Assuming  $\boldsymbol{\gamma}_n$  and  $\boldsymbol{\tau}_n$  are known, determine  $\mathbf{v}^{n+1}$  and  $p^{n+1}$  as the solution to the problem

$$-r\Delta \mathbf{v}^{n+1} + \nabla p^{n+1} = \mathbf{div}(\boldsymbol{\tau}^n - 2r\boldsymbol{\gamma}^n) + \mathbf{f} \quad (2.11)$$

$$\nabla \cdot \mathbf{v}^{n+1} = 0 \quad (2.12)$$

$$\mathbf{v}^{n+1}|_{\Gamma} = \mathbf{v}_B. \quad (2.13)$$

Step 2. Calculate  $\boldsymbol{\gamma}^{n+1}$  as

$$\boldsymbol{\gamma}^{n+1} := \begin{cases} 0, & |\boldsymbol{\tau}^n + 2r\mathbf{D}(\mathbf{v}^{n+1})| < \tau_s \\ \left(1 - \frac{\tau_s}{|\boldsymbol{\tau}^n + 2r\mathbf{D}(\mathbf{v}^{n+1})|}\right) \frac{\boldsymbol{\tau}^n + 2r\mathbf{D}(\mathbf{v}^{n+1})}{2(r + \mu)} & \text{otherwise.} \end{cases} \quad (2.14)$$

Step 3. Calculate  $\boldsymbol{\tau}^{n+1}$  according to (2.10).

If  $\|\boldsymbol{\tau}^{n+1} - \boldsymbol{\tau}^n\| > \varepsilon$  for some given  $\varepsilon > 0$ , then go to Step 1.

The convergence of the algorithm is guaranteed by theorems from [13] for all  $r > 0$ . Concerning the choice of the parameters  $\tilde{r}_n$ , most of the papers known to the authors use the value  $\tilde{r}_n = r/2$  for all  $n$ . Then the main advantage of this algorithm is that the determination of the saddle point of a nondifferentiable functional is reduced to a sequence of standard problems. Steps 2 and 3 are reduced to explicit pointwise calculations. The first step requires the solution of the Stokes equation. Thus, this is a standard problem and can be numerically solved by a number of efficient methods [1, 21].

### 3. Two difference schemes

As was mentioned in the introduction, numerical modelling of Bingham media based on a nonregularized model and variational inequalities mostly uses the finite element method for discretization. In this paper we use two difference schemes for this purpose. One of the difference schemes is a generalization of the well-known MAC scheme on staggered grids. The second scheme uses the same grid (the same nodes) for approximation of all velocity components.

Direct discretization of system (1.1)–(1.3) is difficult, because the domain  $\Omega \setminus \Omega_0$  where the equations of the system are satisfied is initially unknown. Therefore, it is reasonable to construct a difference scheme directly for approximate problems appearing at Steps 1–3 of the algorithm from the previous section. Note that a similar approach was also used in [26, 27] for the construction of a discretization by the finite volume method. Applying this technique, we encounter the following effect. In some cases the difference solution clearly depends on the choice of a particular value of the parameter  $r$ . The parameter  $r$  is not present in the original statement of the problem and is auxiliary. Therefore, such dependence can hardly be assumed acceptable. Below, in Lemma 3.1 we present the condition sufficient for the difference solution not to depend on the parameter  $r$ .

Let  $\Delta_h$ ,  $\mathbf{div}_h$ ,  $\mathbf{D}_h$ ,  $\nabla_h$  approximate the vector differential operators and  $\nabla_h \cdot$  approximate the (scalar) divergence operator in the corresponding spaces of the grid functions and tensor functions. Consider the system of difference equations

$$\nabla_h \cdot \boldsymbol{\tau}_h + \nabla_h p_h = \mathbf{f}_h \quad (3.1)$$

$$\nabla_h \cdot \mathbf{v}_h = 0 \quad (3.2)$$

$$\mathbf{v}_h|_{\Gamma} = \mathbf{v}_B \quad (3.3)$$

and constitutive relations

$$\begin{aligned} \boldsymbol{\tau}_h &= 2\mu \mathbf{D}_h(\mathbf{v}_h) + \tau_s \frac{\mathbf{D}_h(\mathbf{v}_h)}{|\mathbf{D}_h(\mathbf{v}_h)|}, & |\mathbf{D}_h(\mathbf{v}_h)| &\neq 0 \\ |\boldsymbol{\tau}_h| &\leq \tau_s, & |\mathbf{D}_h(\mathbf{v}_h)| &= 0. \end{aligned} \quad (3.4)$$

Examples of difference spaces and operators which assign a specific meaning to system (3.1)–(3.4) will be presented below in this section. Now we prove the following result.

**Lemma 3.1.** *Suppose system of difference equations and constitutive relations (3.1)–(3.4) has only one solution. Let the following condition hold:*

$$\Delta_h = 2\mathbf{div}_h \mathbf{D}_h \quad \text{on } \text{Ker}(\nabla_h \cdot). \quad (3.5)$$

Let the difference analogue of Algorithm (A) possess the property  $\|\boldsymbol{\tau}_h^{n+1} - \boldsymbol{\tau}_h^n\| = 0$  for some sufficiently large  $n$ . Then the sequence of difference functions  $\mathbf{v}_h^{n+1}$ ,  $p_h^{n+1}$ ,  $\boldsymbol{\tau}_h^{n+1}$  has a limit which does not depend on the parameter  $r > 0$  and satisfies the system (3.1)–(3.4).

**Proof.** The equality  $\|\boldsymbol{\tau}_h^{n+1} - \boldsymbol{\tau}_h^n\| = 0$  and (2.10) imply

$$\mathbf{D}_h(\mathbf{v}_h^{n+1}) = \boldsymbol{\gamma}_h^{n+1}. \quad (3.6)$$

Due to (2.12), we have  $\mathbf{v}_h \in \text{Ker}(\nabla_h \cdot)$ . Therefore, system (2.11)–(2.13) together with equalities (3.5) and (3.6) imply

$$\nabla_h \cdot \boldsymbol{\tau}_h^n + \nabla_h p_h^{n+1} = \mathbf{f}_h \quad (3.7)$$

$$\nabla_h \cdot \mathbf{v}_h^{n+1} = 0 \quad (3.8)$$

$$\mathbf{v}_h^{n+1}|_\Sigma = \mathbf{v}_B. \quad (3.9)$$

For convenience sake, introduce the following notation:

$$\mathbf{T}_h = \boldsymbol{\tau}_h^n + 2r \mathbf{D}_h(\mathbf{v}_h^{n+1}). \quad (3.10)$$

Taking into account (3.6), from (2.14) we get

$$\mathbf{D}_h(\mathbf{v}_h^{n+1}) := \begin{cases} 0, & |\mathbf{T}_h| < \tau_s \\ \left(1 - \frac{\tau_s}{|\mathbf{T}_h|}\right) \frac{\mathbf{T}_h}{2(r + \mu)} & \text{otherwise.} \end{cases}$$

This relation is equivalent to the following:

$$\begin{aligned} \mathbf{T}_h &= 2(\mu + r) \mathbf{D}_h(\mathbf{v}_h^{n+1}) + \tau_s \frac{\mathbf{D}_h(\mathbf{v}_h^{n+1})}{|\mathbf{D}_h(\mathbf{v}_h^{n+1})|}, & |\mathbf{D}_h(\mathbf{v}_h^{n+1})| &\neq 0 \\ |\mathbf{T}_h| &\leq \tau_s, & |\mathbf{D}_h(\mathbf{v}_h^{n+1})| &= 0. \end{aligned}$$

According to (3.10), we get

$$\begin{aligned} \boldsymbol{\tau}_h^n &= 2\mu\mathbf{D}_h(\mathbf{v}_h^{n+1}) + \tau_s \frac{\mathbf{D}_h(\mathbf{v}_h^{n+1})}{|\mathbf{D}_h(\mathbf{v}_h^{n+1})|}, \quad |\mathbf{D}_h(\mathbf{v}_h^{n+1})| \neq 0 \\ |\boldsymbol{\tau}_h^n| &\leq \tau_s, \quad |\mathbf{D}_h(\mathbf{v}_h^{n+1})| = 0. \end{aligned} \tag{3.11}$$

Thus, the difference solution  $\mathbf{v}_h^{n+1}, p_h^{n+1}, \boldsymbol{\tau}_h^n$  satisfies the system of difference equations and determining relations (3.7)–(3.9), (3.11), which is equivalent to (3.1)–(3.3), (3.4). Now the assertion of the theorem follows from the assumption of the uniqueness of the difference solution to (3.1)–(3.1), (3.4).

It is well known (see, e.g., [14]) that for stability of discretization methods solving Navier–Stokes equations for an incompressible viscous fluid the fulfillment of the so-called LBB condition (Ladyzhenskaya–Babuska–Brezzi) is important. Below we discuss this condition, as well as consistency condition (3.5) in more detail for each of the considered schemes. Since the Bingham model is in some sense a generalization of the Navier–Stokes model and the Stokes problem is auxiliary in the iterative method considered here, the check of stability in the sense of fulfillment of the LBB condition is a necessary step of the construction of a difference scheme.

### 3.1. Scheme on staggered grids

Consider  $\Omega = (0, 1)^2$ . Assume  $h_x = N_1^{-1}$  and  $h_y = N_2^{-1}$  for given natural  $N_1, N_2$ . Define the following grid domains:

$$\begin{aligned} \bar{\Omega}_1 &= \{x_{ij} = ((i + 1/2)h_x, jh_y) \mid i = 0, \dots, N_1 - 1, j = 0, \dots, N_2\} \\ \bar{\Omega}_2 &= \{x_{ij} = (ih_x, (j + 1/2)h_y) \mid i = 0, \dots, N_1, j = 0, \dots, N_2 - 1\} \\ \Omega_3 &= \{x_{ij} = (ih_x, jh_y) \mid i = 1, \dots, N_1 - 1, j = 1, \dots, N_2 - 1\} \\ \Omega_4 &= \{x_{ij} = ((i + 1/2)h_x, (j + 1/2)h_y) \mid i = 0, \dots, N_1 - 1, j = 0, \dots, N_2 - 1\}. \end{aligned}$$

The mutual position of these grids is illustrated in Fig. 1. Define the spaces of the components of the velocity grid functions

$$\begin{aligned} U_h^0 &= \{u_{ij} := u(x_{ij}) \mid x_{ij} \in \bar{\Omega}_1, u_{0,j} = u_{0,N_1-1} = u_{i,0} = u_{N_2,0} = 0\} \\ V_h^0 &= \{v_{ij} := v(x_{ij}) \mid x_{ij} \in \bar{\Omega}_2, v_{0,j} = v_{0,N_1} = v_{i,0} = v_{N_2-1,0} = 0\}. \end{aligned}$$

By  $U_h, V_h$  we denote the spaces of the grid functions determined only at the ‘internal’ points of  $\Omega_1$  and  $\Omega_2$ . The pressure space is

$$P_h = \left\{ p_{ij} := p(x_{ij}) \mid x_{ij} \in \Omega_3, \sum_{i,j} p_{ij} = 0 \right\}$$

Further, (1,1) and (2,2) components of the rate of deformation tensor ( $\gamma_h^{kk} = \{\gamma_{ij}^{kk}\}$ ) and the deviator of the stress tensor ( $\boldsymbol{\tau}_h^{kk} = \{\tau_{ij}^{kk}\}, k = 1, 2$ ) are given on the grid  $\Omega_3$ ,

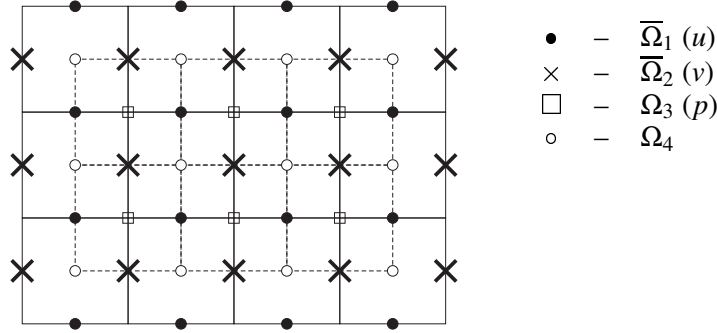


Figure 1. Staggered grids.

whereas mixed (nondiagonal) components  $\gamma_h^{kl} = \{\gamma_{ij}^{kl}\}$ ,  $\tau_h^{kl} = \{\tau_{ij}^{kl}\}$ ,  $k \neq l$ , are given on the grid  $\Omega_4$ . Denote the corresponding space of the grid functions by  $Q_h$ . Thus,  $\boldsymbol{\gamma}_h \in Q_h$  and  $\boldsymbol{\tau}_h \in Q_h$ .

Define the finite-difference analogues of differential operators;  $\Delta_h : U_h^0 \times V_h^0 \rightarrow U_h \times V_h$  is the standard five-point approximation of the Laplace operator on the grids  $\Omega_1$  and  $\Omega_2$ . The grid operators of the gradient  $\nabla_h : P_h \rightarrow U_h \times V_h$  and the divergence  $\nabla_h \cdot : U_h^0 \times V_h^0 \rightarrow P_h$  are

$$(\nabla_h p)_i,j = \left( \frac{p_{i+1,j} - p_{i,j}}{h_x}, \frac{p_{i,j+1} - p_{i,j}}{h_y} \right) \quad (3.12)$$

$$(\nabla_h \cdot \mathbf{v}_h)_{i,j} = \frac{u_{i,j} - u_{i-1,j}}{h_x} + \frac{v_{i,j} - v_{i,j-1}}{h_y}. \quad (3.13)$$

The grid operators of the vector divergence  $\mathbf{div}_h : Q_h \rightarrow U_h \times V_h$  and of the rate of deformation tensor  $\mathbf{D}_h : U_h^0 \times V_h^0 \rightarrow Q_h$  are given in the following way:

$$(\mathbf{div}_h \boldsymbol{\tau}_h)_{i,j} = \left( \frac{\tau_{i+1,j}^{11} - \tau_{i,j}^{11}}{h_x} + \frac{\tau_{i,j}^{12} - \tau_{i,j-1}^{12}}{h_y}, \frac{\tau_{i,j}^{21} - \tau_{i-1,j}^{21}}{h_x} + \frac{\tau_{i,j+1}^{22} - \tau_{i,j}^{22}}{h_y} \right) \quad (3.14)$$

$$(D_h^{11} \mathbf{v}_h)_{i,j} = \frac{u_{i,j} - u_{i-1,j}}{h_x}, \quad (D_h^{22} \mathbf{v}_h)_{i,j} = \frac{v_{i,j} - v_{i,j-1}}{h_y} \quad \text{on } \Omega_3 \quad (3.15)$$

$$(D_h^{12} \mathbf{v}_h)_{i,j} = (D_h^{21} \mathbf{v}_h)_{i,j} = \frac{u_{i,j+1} - u_{i,j}}{2h_y} + \frac{v_{i+1,j} - v_{i,j}}{2h_x} \quad \text{on } \Omega_4. \quad (3.16)$$

Note that relation (2.14) for the calculation of  $\boldsymbol{\gamma}_h$  requires the values of  $|\boldsymbol{\tau}_h + 2r\mathbf{D}_h(\mathbf{v}_h)|$  at the same grid nodes where the corresponding components of  $\boldsymbol{\tau}_h$  and  $\mathbf{D}_h$  are determined. In order to determine the missing components, we use simple averaging over four points. For example, calculating  $\gamma_{i,j}^{11}$ , we have to determine  $\tau_{i,j}^{12}$

and  $D_h^{12}$  at a point  $x_{i,j} \in \Omega_3$ . We set

$$D_h^{12}(x) = D_h^{21}(x) = \frac{1}{4}(D_{i,j}^{12} + D_{i+1,j}^{12} + D_{i,j+1}^{12} + D_{i+1,j+1}^{12})$$

$$\tau_h^{12}(x) = \tau_h^{21}(x) = \frac{1}{4}(\tau_{i,j}^{12} + \tau_{i+1,j}^{12} + \tau_{i,j+1}^{12} + \tau_{i+1,j+1}^{12}), \quad x \in \Omega_3.$$

We similarly calculate auxiliary values at intermediate points for  $D_h^{11}, D_h^{22}, \tau_h^{11}, \tau_h^{22}$ .

The LBB stability condition for this scheme can be written in the following way. Let  $\langle \cdot, \cdot \rangle$  and  $\|\cdot\|$  denote the Euclidean scalar product and norm in  $\mathbb{R}^n$ , respectively. Suppose  $0 < c \leq h_x h_y^{-1} \leq C$  with some absolute constants  $c$  and  $C$ . There exists a constant  $C_0 > 0$  not depending on  $h = \max\{h_x, h_y\}$  and such that

$$\sup_{\mathbf{v}_h \in U_h \times V_h} \frac{\langle p_h, \nabla_h \cdot \mathbf{v}_h \rangle}{\langle -\Delta_h \mathbf{v}_h, \mathbf{v}_h \rangle^{1/2}} \geq C_0 \|p_h\| \quad \forall p_h \in P_h. \tag{3.17}$$

The validity of this condition was proved in [15]. Consider the operator  $S_h = \nabla_h \cdot \Delta_h^{-1} \nabla_h$ . It is easy to check that  $S_h$  is a selfconjugate (with respect to  $\langle \cdot, \cdot \rangle$ ) operator on  $P_h$  and inequality (3.17) is equivalent to

$$C_0 I_h \leq S_h \tag{3.18}$$

where  $I_h$  is the identity operator on  $P_h$ . Estimate (3.18) plays the key role for fast convergence of many iterative methods for the Stokes problem.

It was shown in [18] that for the Stokes problem the scheme has the first order of convergence in grid analogues of the  $H^1$  norm for the velocity and of the  $L^2$  norm for the pressure. In practice, the second order of convergence is observed in the  $L^2$  norm for the velocity. It is worth noting that the first order of approximation of the boundary conditions for  $\mathbf{v}$  can be improved up to the second order [10]. The known results concerning the convergence for the Stokes problem and the second order of approximation of differential operators in (3.14)–(3.16) on the corresponding grids and averaging operators allow us to expect the convergence of the solution of the finite-difference Bingham problem to the solution of the differential problem. It remains to check the well-posedness conditions from Lemma 3.1. Indeed, the validity of (3.5) is checked by direct calculations.

### 3.2. Difference scheme of non-staggered grids

A scheme where the approximation of all velocity components and the rate of deformation tensor components uses non-staggered grids appears more attractive from the viewpoint of implementation convenience and approximation of boundary conditions. Below we construct such a scheme and discuss the way to overcome difficulties arising from the LBB instability of that scheme.

As in the previous section, consider  $\Omega = (0, 1)^2$  and assume  $h_x = N_1^{-1}$ ,  $h_y = N_2^{-1}$ . Define the following grid domains:

$$\begin{aligned}\bar{\Omega}_1 &= \{x_{ij} = (ih_1, jh_2) \mid i = 0, \dots, N_1, j = 0, \dots, N_2\} \\ \Omega_2 &= \left\{x_{ij} = \left(\left(i + \frac{1}{2}\right)h_1, \left(j + \frac{1}{2}\right)h_2\right) \mid i = 0, \dots, N_1 - 1, j = 0, \dots, N_2 - 1\right\}.\end{aligned}$$

Define the spaces of the components of velocity and pressure grid functions:

$$\begin{aligned}U_h^0 &= \{\mathbf{u}_{i,j} = (u_{ij}, v_{ij}) := (u(x_{ij}), v(x_{ij})) \mid x_{ij} \in \bar{\Omega}_1, \mathbf{u}_{0,j} = \mathbf{u}_{0,N_1} = \mathbf{u}_{i,0} = \mathbf{u}_{N_2,0} = \mathbf{0}\} \\ P_h &= \{p_{ij} := p(x_{ij}) \mid x_{ij} \in \Omega_2, \sum_{i,j} p_{ij} = 0\}.\end{aligned}$$

By  $U_h$  we denote the spaces of the grid vector functions determined only at ‘internal’ points of  $\Omega_1$ . All components of the rate of deformation tensor ( $\boldsymbol{\gamma}_h = \{\boldsymbol{\gamma}_{ij}\}$ ) and the deviator of the stress tensor ( $\boldsymbol{\tau}_h = \{\boldsymbol{\tau}_{ij}\}$ ) are given on the grid  $\Omega_2$ . Denote the corresponding space of the grid tensor functions by  $Q_h$ .

Define the grid operators of the gradient  $\nabla_h : P_h \rightarrow U_h$  and divergence  $\nabla_h \cdot : U_h^0 \rightarrow P_h$ :

$$\begin{aligned}(\nabla_h p)_{i,j} &= \left( \frac{p_{i,j} - p_{i-1,j} + p_{i,j-1} - p_{i-1,j-1}}{2h_x}, \frac{p_{i,j} - p_{i,j-1} + p_{i-1,j} - p_{i-1,j-1}}{2h_y} \right) \\ (\nabla_h \cdot \mathbf{v}_h)_{i,j} &= \frac{u_{i+1,j+1} - u_{i,j+1} + u_{i+1,j} - u_{i,j}}{2h_x} + \frac{v_{i+1,j+1} - v_{i+1,j} + v_{i,j+1} - v_{i,j}}{2h_y}.\end{aligned}$$

The grid operators of vector divergence  $\mathbf{div}_h : Q_h \rightarrow U_h$  and the rate of deformation tensor  $\mathbf{D}_h : U_h^0 \rightarrow Q_h$  are defined in the following way:

$$\begin{aligned}(\mathbf{div}_h \boldsymbol{\tau}_h)_{i,j} &= \left( \frac{\tau_{i,j}^{11} - \tau_{i-1,j}^{11} + \tau_{i,j-1}^{11} - \tau_{i-1,j-1}^{11}}{2h_x} + \frac{\tau_{i,j}^{12} - \tau_{i,j-1}^{12} + \tau_{i-1,j}^{12} - \tau_{i-1,j-1}^{12}}{2h_y}, \right. \\ &\quad \left. \frac{\tau_{i,j}^{21} - \tau_{i-1,j}^{21} + \tau_{i,j-1}^{21} - \tau_{i-1,j-1}^{21}}{2h_x} + \frac{\tau_{i,j}^{22} - \tau_{i,j-1}^{22} + \tau_{i-1,j}^{22} - \tau_{i-1,j-1}^{22}}{2h_y} \right) \\ (D_h^{11} \mathbf{v}_h)_{i,j} &= \frac{u_{i+1,j+1} - u_{i,j+1} + u_{i+1,j} - u_{i,j}}{2h_x} \\ (D_h^{22} \mathbf{v}_h)_{i,j} &= \frac{v_{i+1,j+1} - v_{i+1,j} + v_{i,j+1} - v_{i,j}}{2h_y} \\ (D_h^{12} \mathbf{v}_h)_{i,j} &= (D_h^{21} \mathbf{v}_h)_{i,j} = \frac{u_{i+1,j+1} - u_{i+1,j} + u_{i,j+1} - u_{i,j}}{4h_y} \\ &\quad + \frac{v_{i+1,j+1} - v_{i,j+1} + v_{i+1,j} - v_{i,j}}{4h_x}.\end{aligned}$$

The approximation of the Laplace operator is needed to satisfy the condition of consistency for the operators  $\Delta_h$ ,  $\mathbf{div}_h$ ,  $\mathbf{D}_h$ , and  $\nabla_h \cdot$  from Lemma 3.1. For  $\mathbf{x}_h$  such that  $\nabla_h \cdot \mathbf{v}_h = 0$  one can easily verify:

$$\begin{aligned} \nabla_h \cdot (\mathbf{D}_h \mathbf{v}_h)_{i,j} &= \frac{1}{4h_1^2} (v_{i+1,j+1} - 2v_{i,j+1} + v_{i-1,j+1} + 2v_{i+1,j} - 4v_{i,j} \\ &\quad + 2v_{i-1,j} + v_{i+1,j-1} - 2v_{i,j-1} + v_{i-1,j-1}) \\ &\quad + \frac{1}{4h_2^2} (v_{i+1,j+1} + 2v_{i,j+1} + v_{i-1,j+1} - 2v_{i+1,j} - 4v_{i,j} \\ &\quad - 2v_{i-1,j} + v_{i+1,j-1} + 2v_{i,j-1} + v_{i-1,j-1}) \\ &=: (\Delta_h \mathbf{v}_h)_{ij}. \end{aligned}$$

Note that for  $h_1 = h_2 = h$ , from the nine-point approximation we obtain the so-called ‘shift’ approximation:

$$(\Delta_h \mathbf{v}_h)_{i,j} = \frac{v_{i-1,j-1} + v_{i+1,j-1} + v_{i+1,j+1} + v_{i-1,j+1} - 4v_{i,j}}{2h^2}. \quad (3.19)$$

Note that in the case of the common five-point stencil for  $\Delta_h$ , numerical solutions of the problem with fixed  $\tau_s$  and  $\mu$  actually demonstrate the dependence of the difference solution on  $r$  (this is primarily indicated by the sizes of the rigid zones).

The scheme constructed here is LBB-unstable for the Stokes problem. Indeed, it is sufficient to notice that the grid gradient operator has a nontrivial kernel in the space  $P_h$ :

$$\text{Ker}(\nabla_h) = \text{span}(p^1, p^2), \quad p_{i,j}^1 = (-1)^{i+j} - 1, \quad p_{i,j}^2 = (-1)^{i+j+1} - 1$$

therefore, the operator  $S_h$  has a nontrivial kernel in  $P_h$  and inequality (3.18) holds only for  $C_0 = 0$ . Therefore, the finite difference LBB stability condition (3.17) does not hold. Moreover, in the three-dimensional case the dimension of the kernel grows with a decreasing  $h$  (see [17]). This is the reason why the schemes on non-staggered grids are less popular than the schemes on staggered grids in computational fluid dynamics for incompressible fluids. Note that some authors (see [6] and the references therein) use non-staggered grids together with splitting schemes for the calculation of viscous incompressible flows. A special term has been introduced in those papers into equations for the pressure; this term is in some sense equivalent to adding a biharmonic operator to the continuity equation. The magnitude of this term depends both on the spatial mesh size and the time step. This poses the smallness condition onto the time step, which makes this method not very attractive for the calculation of steady or slowly varying flows. In this paper we propose another stabilization approach for the scheme on non-staggered grids.

The similar issue of the LBB instability appears in the finite element method applied to the Stokes problem; for example, when one uses polynomials of the same degree for approximation of  $\mathbf{u}$  and  $p$ . In this case *stabilized* methods are constructed

on the basis of the variational Petrov–Galerkin method and the obtained schemes possess stability and the optimal order of convergence. As the result, LBB-unstable finite elements have become widespread in practice and have a substantial mathematical foundation, see, e.g., review [5] and the references therein.

In recent paper [4], a method of stabilization of LBB-unstable elements of a low order was proposed, which was not explicitly based on a variational statement of the Stokes problem. Since the considered difference schemes have analogies with finite element methods of low orders (in particular, this was used in [18] for analysis of convergence of the MAC scheme), it is reasonable to adapt this approach to stabilization of a difference scheme on non-staggered grids. Thus, it is natural to associate the difference scheme considered in this section with the finite element method  $Q_1 - Q_0$  (piecewise-bilinear approximation for velocity and piecewise-constant approximation for pressure) with respect to the grid  $\Omega_1$ . This finite element method is LBB-unstable. A mathematical base for the construction of stable schemes is the validity of the following ‘weak’ LBB inequality for elements  $Q_1 - Q_0$  (see [4, 11, 24]):

$$\sup_{\mathbf{u}_h \in U_h} \frac{(p_h, \nabla \cdot \mathbf{u}_h)}{\|\nabla \mathbf{u}_h\|} \geq C_0 \|p_h\| - C_1 \left( h \sum_{\tau} \int_{\tau} [p_h]^2 ds \right)^{1/2} \quad \forall p_h \in P_h \quad (3.20)$$

with some constants  $C_0, C_1$  not depending on  $h$ . In the latter term the summation is taken over all internal faces (or edges in the case  $\Omega \in \mathbb{R}^2$ ) of the triangulation elements,  $[p_h]$  denotes the jump in  $p_h$  over a face. Thus, the stabilization of the method is reduced to the addition (in one or another way) of the term  $-G(p)$ , such that  $G(p) \geq h^{1/2} \|[p_h]_{\tau}\|$  to the Lagrangian of the problem; and the approximation order of the scheme on smooth solutions remains possibly optimal. It has been shown in [4] that for stabilization of  $Q_1 - Q_0$  elements it is sufficient to augment the Lagrangian with the term  $-\int_{\Omega} (p - \Pi p)^2 dx$ , where  $\Pi$  is some operator of local interpolation from  $P_h$  into the space of piecewise-bilinear functions.

For stabilization of the scheme on non-staggered grids, we define an operator  $\Pi_h : P_h \rightarrow R_h$ , where  $R_h$  is the space of grid functions determined on  $\bar{\Omega}_1$ . Let  $x_{ij} \in \bar{\Omega}_1$ . Denote

$$\omega(x_{ij}) = \{x_{kl} \in \Omega_2 \mid |x_{kl} - x_{ij}| = (h_x^2 + h_y^2)^{1/2}/2\}$$

then

$$(\Pi_h p_h)_{ij} = |\omega(x_{ij})|^{-1} \sum_{x_{kl} \in \omega(x_{ij})} p_{kl}.$$

The operator  $\Pi_h$  can be considered as the grid ‘interpolation’ of a function given on the grid  $\Omega_2$  by a function given on the grid  $\Omega_1$ .  $\Pi_h$  can be naturally defined in the case of nonuniform grids. Let  $\Pi_h^*$  be the adjoint operator with respect to the Euclidean scalar product. Assume

$$G_h := (I_h - \Pi_h^* \Pi_h), \quad G_h : P_h \rightarrow P_h.$$

In the nonstabilized scheme on non-staggered grids the continuity equation  $\nabla \cdot \mathbf{v} = 0$  is approximated on the grid  $\Omega_2$  in the following way:

$$\nabla_h \cdot \mathbf{v}_h + G_h p_h = 0.$$

For the scheme constructed here, the system of algebraic equations for solving the Stokes problem (Step 1 in the algorithm from Section 2) takes the form

$$\begin{pmatrix} A & B \\ B^T & -C \end{pmatrix} \begin{pmatrix} \mathbf{v} \\ p \end{pmatrix} = \begin{pmatrix} \mathbf{f} \\ \mathbf{g} \end{pmatrix}.$$

The matrix is sparse and has a block structure. By analogy with (3.18), the stability condition for the stabilized scheme can be written in the operator form:

$$C_0 I_h \leq \nabla_h \cdot \Delta_h^{-1} \nabla_h - G_h \quad \text{on } P_h \tag{3.21}$$

or in the matrix form  $C_0 I \leq BA^{-1}B^T + C$  with some constant  $C_0 > 0$  not depending on  $h$ .

Below we present the results of numerical experiments for the Stokes problem demonstrating that the proposed scheme is stable and has the second order of convergence for  $\mathbf{u}$  and the first order of convergence for  $p$  in the grid analogue of the  $L_2$ -norm. Mathematical analysis of this scheme including checking of (3.21) will be the subject of a separate paper. Here we only point out the following simple property of the operator  $G_h$ , which can be verified by direct calculations.

**Lemma 3.2.** *Let the grid be uniform, then  $G_h = \frac{1}{4}h^2\Delta_h^p$ , where  $\Delta_h^p$  is some approximation of the Laplace operator on a nine-point stencil with Neumann boundary conditions of the second order on  $\Omega_2$ .*

#### 4. Numerical results

Consider the Stokes problem on  $(0, 1)^2$  with known analytic solutions:

$$\begin{aligned} \mathbf{v} &= \left( \frac{1}{4\pi^2} (1 - \cos 2\pi x) \sin 2\pi y, \frac{1}{4\pi^2} \sin 2\pi x (1 - \cos 2\pi y) \right) \\ p &= \frac{1}{\pi} \sin 2\pi x \sin 2\pi y \end{aligned} \tag{4.1}$$

and

$$\begin{aligned} v &= \left( 1 - \cos \left( \frac{2\pi(e^{R_1 x} - 1)}{e^{R_1} - 1} \right) \right) \sin \left( \frac{2\pi(e^{R_2 y} - 1)}{e^{R_2} - 1} \right) \frac{R_2}{2\pi} \frac{e^{R_2 y}}{(e^{R_2} - 1)} \\ u &= \sin \left( \frac{2\pi(e^{R_1 x} - 1)}{e^{R_1} - 1} \right) \left( 1 - \cos \left( \frac{2\pi(e^{R_2 y} - 1)}{e^{R_2} - 1} \right) \right) \frac{R_1}{2\pi} \frac{e^{R_1 x}}{(e^{R_1} - 1)} \\ p &= R_1 R_2 \sin \left( \frac{2\pi(e^{R_1 x} - 1)}{e^{R_1} - 1} \right) \sin \left( \frac{2\pi(e^{R_2 y} - 1)}{e^{R_2} - 1} \right) \frac{e^{R_1 x} e^{R_2 y}}{(e^{R_1} - 1)(e^{R_2} - 1)} \end{aligned} \tag{4.2}$$

for  $R_1 = 4.2985, R_2 = 0.1$ . The solution from (4.2) imitates a ‘vortex’ in the cavity, the center of the vortex has the coordinates  $x = (1/R_1) \log((\exp(R_1) + 1)/2), y =$

**Table 1.**

Convergence of the difference solution and the number of iterations, example (4.1).

$h$	$ e_h _{L_2}$	$\frac{ e_h _{L_2}}{ e_{2h} _{L_2}}$	$\log_2 \frac{ e_h _{L_2}}{ e_{2h} _{L_2}}$	$ r_h _{L_2}$	$\frac{ r_h _{L_2}}{ r_{2h} _{L_2}}$	$\log_2 \frac{ r_h _{L_2}}{ r_{2h} _{L_2}}$	#iter
Scheme 1 (MAC)							
$h = \frac{1}{16}$	$1.37 \times 10^{-3}$	3.61	1.85	$4.57 \times 10^{-2}$	1.97	0.97	16
$h = \frac{1}{32}$	$3.79 \times 10^{-4}$	3.79	1.92	$2.31 \times 10^{-2}$	1.99	0.9	19
$h = \frac{1}{64}$	$9.98 \times 10^{-5}$			$1.16 \times 10^{-2}$			25
Scheme 2 (non-staggered grids)							
$h = \frac{1}{16}$	$1.24 \times 10^{-3}$	3.68	1.88	$4.43 \times 10^{-2}$	1.99	0.99	15
$h = \frac{1}{32}$	$3.37 \times 10^{-4}$	3.86	1.95	$2.22 \times 10^{-2}$	2.00	1.00	15
$h = \frac{1}{64}$	$8.73 \times 10^{-5}$			$1.11 \times 10^{-2}$			16

**Table 2.**

Convergence of the difference solution and the number of iterations, example (4.2).

$h$	$ e_h _{L_2}$	$\frac{ e_h _{L_2}}{ e_{2h} _{L_2}}$	$\log_2 \frac{ e_h _{L_2}}{ e_{2h} _{L_2}}$	$ r_h _{L_2}$	$\frac{ r_h _{L_2}}{ r_{2h} _{L_2}}$	$\log_2 \frac{ r_h _{L_2}}{ r_{2h} _{L_2}}$	#iter
Scheme 1 (MAC)							
$h = \frac{1}{16}$	$1.29 \times 10^{-3}$	3.78	1.91	$4.81 \times 10^{-2}$	1.95	0.96	20
$h = \frac{1}{32}$	$3.41 \times 10^{-4}$	3.87	1.95	$2.46 \times 10^{-2}$	1.98	0.98	26
$h = \frac{1}{64}$	$8.80 \times 10^{-5}$			$1.24 \times 10^{-2}$			29
Scheme 2 (non-staggered grids)							
$h = \frac{1}{16}$	$1.35 \times 10^{-3}$	3.86	1.94	$4.83 \times 10^{-2}$	1.97	0.97	19
$h = \frac{1}{32}$	$3.49 \times 10^{-4}$	3.93	1.97	$2.45 \times 10^{-2}$	1.99	0.9	19
$h = \frac{1}{64}$	$8.88 \times 10^{-5}$			$1.23 \times 10^{-2}$			20

**Table 3.**The number of nonlinear iterations  
( $h = 1/32, r = 1$ ).

$\tau_s$	1	2	5
scheme 1	165	345	487
scheme 2	152	307	498

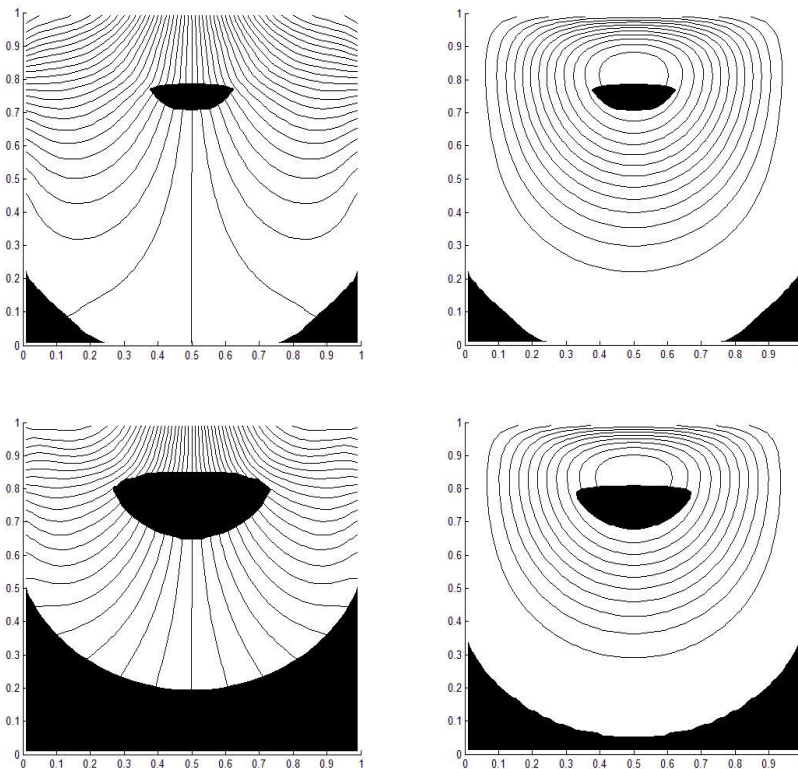


**Figure 2.** Isobars, streamlines, and rigid zones for  $\tau_s = 1$  (top). Isobars and rigid zones for  $\tau_s = 5$  (left, bottom), streamlines and rigid zones for  $\tau_s = 2$  (right, bottom). The scheme on non-staggered grids,  $h = 1/64$ .

$(1/R_2) \log((\exp(R_2) + 1)/2)$ . Thus, near the right part of the boundary the solution has a boundary layer (see [3]).

Tables 1 and 2 present the norms of the errors in the velocity  $\mathbf{e}_h = \mathbf{v}|_{\Omega_1} - \mathbf{v}_h$  and in the pressure  $r_h = p|_{\Omega_2} - p_h$  for the MAC scheme and the stabilized scheme on non-staggered grids and also the number of iterations in the Uzawa – conjugate gradient method necessary for decreasing the residual norm up to  $10^{-9}$  (the method consists in solution of the equation for the pressure with the matrix  $BA^{-1}B^T + C$  (for Scheme 1  $C = 0$ ) by the method of conjugate gradients. The system of equations with the matrix  $A$  is solved exactly at each step). For Scheme 2 we note the second order of convergence for the velocity and the first order for the pressure and also the fact that the number of iterations in the Uzawa-CG method does not actually depend on the mesh size. In general the results for the stabilized scheme on non-staggered grids are not worse than for the MAC scheme.

The fulfillment of the consistency condition for the operators  $\Delta_h$ ,  $\mathbf{div}_h$ ,  $\mathbf{D}_h$ , and  $\nabla_h \cdot$  from Lemma 3.1 and the optimal convergence order of the scheme for the linear problem allow us to use these schemes for the calculation of the Bingham model.

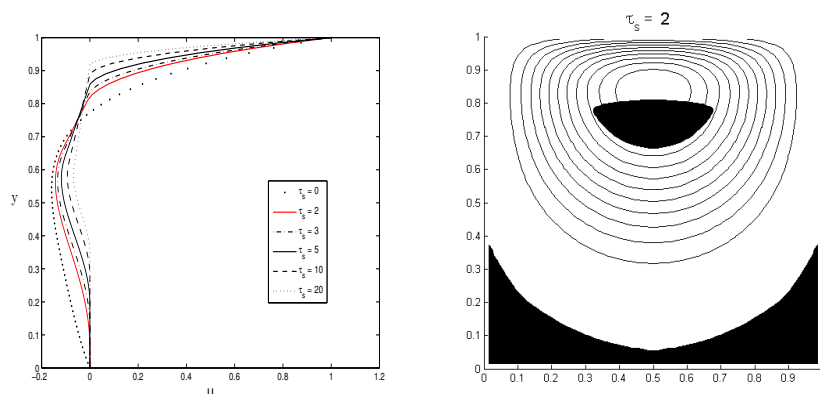


**Figure 3.** Profiles of  $u(0.5, y)$  for various  $\tau_s$  (left) and streamlines for  $\tau_s = 3$  (right). The scheme on staggered grids,  $h = 1/64$ .

As a numerical test for Bingham media, consider the problem of a flow in a cavity. Assume  $\Omega = (0, 1) \times (0, 1)$ ,  $\mathbf{f} = 0$ , the boundary conditions are given as

$$\mathbf{v}_B(\mathbf{x}) := \begin{cases} 0, & x \in \Gamma \setminus \Gamma_B \\ \{16(x_1^2(1-x_1)^2), 0\}, & x \in \Gamma_B \end{cases}$$

where  $\Gamma_B = \{\mathbf{x} \mid \mathbf{x} = (x_1, x_2), 0 < x_1 < 1, x_2 = 1\}$ . This problem is a standard test in computational fluid dynamics. Our choice of the nonzero horizontal velocity component corresponds to the so-called regularized cavity problem. In order to obtain a numerical solution, we use the algorithm from Section 2. The number of iterations necessary to satisfy the given criterion ( $\|\boldsymbol{\tau}^{n+1} - \boldsymbol{\tau}^n\| < 10^{-4}$ ) is approximately the same for both difference schemes and essentially grows under an increasing yield point  $\tau_s$ , see Table 3. In each iteration of the method we solve the Stokes problem by the iterative method from the previous section.

In order to determine rigid zones in the obtained difference solution, we apply the Mises criterion ( $|\boldsymbol{\tau}| = \tau_s$ ). Figure 2 shows the rigid zones and streamlines for various values of the yield limit  $\tau_s$ . Figure 3 (left) shows the profile of the first velocity vector component along the line  $x = 0.5$  for various values of  $\tau_s$ . Figure 3 (right) presents pressure isolines for  $\tau_s = 2$ . The results obtained by schemes 1 and 2 do not visually differ. Thus, the results in Fig. 2 are obtained by using the difference scheme on non-staggered grids and those in Fig. 3 are obtained using staggered grids. The form and shape of the rigid zones obtained in our calculations are in good agreement with the results from [8, 16, 23]; the velocity profiles match the results of [25]. We think that the ‘superposition’ of the streamlines of the obtained solutions onto the central rigid zone is not physical. But the same pattern is observed in the results presented in [8, 16, 25]. This can be probably explained by the approximation error permitting a (very slow) flow within the rigid zones.

## Acknowledgements

The authors are grateful to L. V. Muravleva for the problem statement and fruitful discussions and to R. Čiegis, O. Iliev, R. Lazarov, and P. N. Vabishchevich for their useful comments.

## References

1. M. Benzi, G. H. Golub, and J. Liesen, Numerical solution of saddle point problems. *Acta Numerica* (2005) **14**, 1–137.
2. M. Bercovier and M. Engelman, A finite element method for incompressible non-Newtonian flows. *J. Comp. Phys.* (1980) **36**, 313–326.
3. S. Berrone, Adaptive discretization of the Navier Stokes equations by stabilized finite element methods. *Comp. Meth. Appl. Mech. Engrg.* (2001) **190**, 4435–4455.
4. P. B. Bochev, C. R. Dohrmann, and M. D. Gunzburger, Stabilization of low-order mixed finite elements for the Stokes equations. *SIAM J. Numer. Anal.* (2006) **44**, 82–101.
5. M. Braack, E. Burman, V. John, and G. Lube, Stabilized finite element methods for the generalized Oseen problem. *Comp. Meth. Appl. Mech. Engrg.* (2007) **196**, 853–866.
6. A. G. Churbanov, A. N. Pavlov, and P. N. Vabishchevich, Operator-splitting method for incompressible Navier–Stokes equations on non-staggered grids. Part I: First-order schemes. *Int. J. Numer. Meth. Fluids* (1995) **21**, 617–640.
7. E. J. Dean and R. Glowinski, Operator-splitting methods for the simulation of Bingham viscoplastic flow. *Chin. Ann. Math.* (2002) **B 23**, 187–204.
8. E. J. Dean, R. Glowinski, and G. Guidoboni, On the numerical simulation of Bingham viscoplastic flow: Old and New results. *J. Non-Newtonian Fluid Mech.* (2007) **142**, 36–62.
9. G. Duvaut and J.-L. Lions, *Inequalities in Mechanics and Physics*. Springer, New York etc. 1976.
10. C. A. J. Fletcher, *Computational Techniques for Fluid Dynamics, Vol. 2*. Springer, Berlin, 1991.
11. L. P. Franca and R. Stenberg, Error analysis of some Galerkin least-squares methods for the elasticity equations. *SIAM J. Numer. Anal.* (1991) **28**, 1680–1697.
12. R. Glowinski, J.-L. Lions, and R. Trémoières, *Numerical Analysis of Variational Inequalities*. North-Holland, Amsterdam, 1981.
13. R. Glowinski, *Numerical Methods for Nonlinear Variational Problems*. Springer, New York, 1984.
14. V. Girault and P. A. Raviart, *Finite Element Methods for Navier-Stokes Equations*. Springer, Berlin, 1986.
15. G. M. Kobel’kov and V. D. Valedinsky, On the inequality  $\|p\|_{L_2} \leq c\|\nabla p\|_{W_2^{-1}}$  and its finite dimensional analog. *Sov. J. Numer. Anal. Math. Modelling* (1986) **1**, No. 3, 189–200.
16. E. Mitsoulis and Th. Zisis, Flow of Bingham plastics in a lid-driven cavity. *J. Non-Newtonian Fluid Mech.* (2001) **101**, 173–180.
17. E. A. Muravleva, On the kernel of the discrete gradient operator. *Numer. Meth. Prog.* (2008) **1**, 93–100.
18. R. A. Nicolaides, Analysis and convergence of the MAC scheme I. The linear problem. *SIAM J. Numer. Anal.* (1992) **29**, 1579–1591.

19. E. J. O'Donovan and R. I. Tanner, Numerical study of the Bingham squeeze film problem. *J. Non-Newtonian Fluid Mech.* (1984) **15**, 75–83.
20. T. C. Papanastasiou, Flows of materials with yield. *J. Rheol.* (1987) **31**, No. 5, 385–404.
21. J. Peters, V. Reichelt, and A. Reusken, Fast iterative solvers for discrete Stokes equations. *SIAM J. Sci. Comp.* (2005) **27**, 646–666.
22. N. Roquet and P. Saramito, An adaptive finite element method for Bingham fluid flow around a cylinder. *Comp. Meth. Appl. Mech. Engrg.* (2003) **192**, 3317–3341.
23. F. J. Sanchez, Application of a first-order operator splitting method to Bingham fluid flow simulation. *Comp. Math. Appl.* (1998) **36**, No. 3, 71–86.
24. R. Stenberg, Error analysis of some finite element methods for the Stokes problem. *Math. Comp.* (1990) **54**, 495–508.
25. D. Vola, L. Boscardin, and J. C. Latche, Laminar unsteady flows of Bingham fluids: a numerical strategy and some benchmark results. *J. Comp. Phys.* (2003) **187**, 441–456.
26. G. Vinay, A. Wachs, and J. F. Agassant, Numerical simulation of non-isothermal viscoplastic waxy crude oil flows. *J. Non-Newtonian Fluid Mech.* (2005) **128**, 144–162.
27. A. Wachs, Numerical simulation of steady Bingham flow through an eccentric annular cross-section by distributed Lagrange multiplier/fictitious domain and augmented Lagrangian methods. *J. Non-Newtonian Fluid Mech.* (2007) **142**, 183–198.